JOURNAL OF SYNCHROTRON RADIATION
ISSN 1600-5775

A simple and compact scheme to enhance the brightness of self-amplified spontaneous emission free-electron-lasers[1]

Eduard Prat* and Sven Reiche

Paul Scherrer Institut, CH-5232 Villigen PSI, Switzerland. *Correspondence e-mail: eduard.prat@psi.ch

Received 9 October 2018
Accepted 21 April 2019

Edited by M. Yabashi, RIKEN SPring-8 Center, Japan

[1] This article will form part of a virtual special issue on X-ray free-electron lasers.

Keywords: free-electron-laser; coherence; brightness; compact undulator beamline; simulations.

A simple and compact scheme that enhances the brightness of self-amplified spontaneous-emission (SASE) free-electron lasers is presented. The method combines the high-brightness SASE scheme and the optical klystron concept to increase the temporal coherence of the produced radiation and to reduce the required length of the undulator beamline at the same time. The scheme is very simple and only requires compact chicanes between the modules of the undulator beamline. Simulations show that, in comparison with SASE, the brightness can be improved by up to a factor of ten and the required length to achieve saturation can be reduced by 20% or more.

1. Introduction

X-ray free-electron lasers (FELs) are leading-edge research instruments employed in multiple research fields such as biology, chemistry and material science. FELs produce high-power transversely coherent radiation with wavelengths down to the sub-ångström level and pulse durations of tens of femtoseconds and shorter (Pellegrini *et al.*, 2016; Emma *et al.*, 2010; Ishikawa *et al.*, 2012; Kang *et al.*, 2017; Ackermann *et al.*, 2007; Allaria *et al.*, 2012, 2013). Most of the current FEL facilities are based on self-amplified spontaneous emission (SASE) (Kondratenko & Saldin, 1980; Bonifacio *et al.*, 1984) which starts from incoherent radiation based on the inherent electrons' shot noise of the arrival time at the undulator entrance. Typically, the generated SASE radiation has limited temporal coherence, given the attainable relative bandwidth of the order of 10^{-3} or 10^{-4} for X-ray FELs.

There are various methods to improve the longitudinal coherence of the SASE-FEL pulses. One possibility is to start the FEL process with a coherent seed signal larger than the shot noise power of the electron beam. The seed can be an external laser or monochromated SASE radiation produced in an early stage. Laser-based seeding can consist of seeding directly with a high-harmonic-generation source (Ferray *et al.*, 1988) or by employing more sophisticated schemes with magnetic chicanes and modulators, such as for example in the high-gain harmonic generation (Yu, 1991) or the echo-enabled harmonic generation (Stupakov, 2009) methods. External seeding based on the high-gain harmonic generation scheme has produced nearly fully coherent FEL radiation for extreme ultraviolet (Allaria *et al.*, 2012) and soft X-rays (Allaria *et al.*, 2013). These schemes are currently limited to the wavelength range of a few nanometres, and aiming for smaller wavelengths may be difficult due to the reduced laser power at short wavelengths and noise amplification issues (Saldin *et al.*, 2002). The second type of seeding, called self-seeding (Feld-

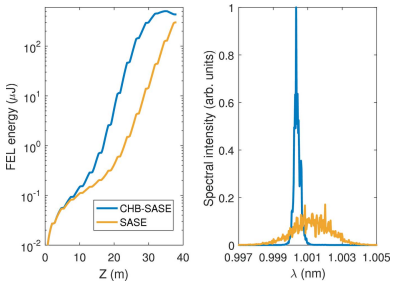

haus *et al.*, 1997; Saldin *et al.*, 2001; Geloni & Saldin, 2010), has been demonstrated for soft and hard X-rays (Ratner *et al.*, 2015; Amann *et al.*, 2012). Self-seeding can produce close to transform-limited FEL radiation but it requires an undulator beamline longer than for SASE, a monochromator and an electron bypass line.

A different approach is to increase the FEL slippage length, *i.e.* the cooperation length between the electron and photon beams. Several methods have been proposed to increase the slippage: the high-brightness SASE (HB-SASE) scheme [also called improved SASE or iSASE (Wu *et al.*, 2013*b*)] uses magnetic chicanes between the undulator modules to imprint delays on the electron beam (McNeil *et al.*, 2013); the purified SASE method employs undulator modules tuned at the subharmonic of the wavelength of interest (Xiang *et al.*, 2013); harmonic lasing schemes are analogous to purified SASE but propose to start the FEL process already with an undulator section tuned to a subharmonic of the wavelength of interest and to continue in a second stage tuned to the wavelength of interest, both for SASE (Schneidmiller & Yurkov, 2012; Schneidmiller *et al.*, 2017) and self-seeding configurations (Geloni *et al.*, 2011, 2015; Prat & Reiche, 2018). The most promising slippage-enhancing scheme is HB-SASE. Similar to the seeding methods, HB-SASE can potentially generate transform-limited FEL pulses if the chicanes between short undulator modules are isochronous. Compared with the seeding schemes, HB-SASE has a single-stage configuration, does not require an external laser or a monochromator, and can work at any repetition rate. HB-SASE has been demonstrated with a limited setup (Wu *et al.*, 2013*a*) and is planned to be further exploited at future facilities such as CLARA (Clarke *et al.*, 2014) and the soft X-ray beamline of SwissFEL (Ganter, 2017; Prat *et al.*, 2016).

Here we propose a method that combines the HB-SASE idea with the optical klystron effect (Vinokurov & Skrinsky, 1977; Saldin *et al.*, 2003; Ding *et al.*, 2006; Penco *et al.*, 2015) to improve the brightness of the SASE-FEL radiation in a more compact beamline. Since the brightness is increased but the required undulator beamline is also reduced, we call this new scheme *compact high-brightness SASE* (CHB-SASE). The method is simple and it only requires small chicanes in the inter-undulator sections of the FEL beamline. In Section 2, after outlining the concept and limitations of the HB-SASE and the optical klystron schemes, we will describe the CHB-SASE method. In Section 3 we will present simulation results showing that the scheme can improve the FEL brightness up to a factor of ten and, at the same time, reduce the saturation length by at least 20%.

2. Description of the method

CHB-SASE combines the HB-SASE and the optical klystron concepts. Both methods use magnetic chicanes placed between the undulator modules of the FEL facility. Before describing the HB-SASE and optical klystron schemes, we briefly need to explain the difference between standard and isochronous chicanes. Standard chicanes consist of only dipole magnets and have two physical effects: they delay the electrons with respect to the photons and they introduce longitudinal dispersion to the electron beam. These two effects are coupled, the longitudinal dispersion being approximately twice the delay. A non-zero longitudinal dispersion implies that the longitudinal position of an electron will change after the chicane depending on its energy. Due to its longitudinal dispersion, a standard chicane will alter the microbunching of the electron beam and therefore will influence the FEL process. By contrast, isochronous chicanes only delay the electron beam and have no longitudinal dispersion; *i.e.* the change of longitudinal position of an electron within the chicane is independent of the electron's energy and therefore the FEL microbunching is not affected. Isochronous chicanes require at least three quadrupole magnets to cancel the longitudinal dispersion and are significantly longer than standard chicanes.

The fundamental idea of HB-SASE is to increase the FEL cooperation length by delaying the electrons with respect to the photon beam using magnetic chicanes. With frequent shifts the radiation of *hot spots* (locations with a high density of electrons and thus enhanced emission) is spread over the full bunch length, delocalizing the strong emission which otherwise would form a local spike in normal SASE radiation. For best performance, the HB-SASE scheme requires isochronous magnetic chicanes not affecting the microbunching. Standard chicanes with residual longitudinal dispersion will change the electron microbunching and, consequently, the coherence improvement with respect to SASE will be limited to approximately a factor of ten (McNeil *et al.*, 2013). The undulator module length should ideally be shorter than the FEL field gain length to allow for frequent delays and thus larger slippage: McNeil *et al.* (2013) showed that the brightness increase with respect to SASE is approximately 100 when the module length is half of the gain length, 50 when the module length is equal to the gain length, and 10 when the module length is twice the gain length. The field gain length of a typical X-ray FEL facility such as SwissFEL is around 2 m to 4 m, therefore an optimum HB-SASE performance requires undulator modules with a length of about 2 m or shorter.

In summary, an optimum HB-SASE scheme demands short undulator modules and long chicanes with several quadrupole magnets, reducing the filling factor (ratio between the length of the inter-undulator section and the module length) and therefore decreasing the efficiency of the undulator beamline. Moreover, the optics along the undulator beamline will typically be highly disrupted due to the strong quadrupole magnets of the isochronous chicanes. For all these reasons, it is rather impractical for a real FEL facility to implement the HB-SASE scheme in its optimal configuration.

The distributed optical klystron concept consists of accelerating the FEL process by speeding up the formation of microbunching using the longitudinal dispersion of standard chicanes between the undulator modules. The saturation length can be significantly improved using the optical klystron effect, *e.g.* simulations performed for the soft X-ray beamline of SwissFEL showed a reduction in saturation length of about

30% (Prat *et al.*, 2016). However, operating exactly at the optimum delay for the distributed optical klystron would deteriorate the radiation spectrum via the formation of sidebands: hot spots are reproduced with a regular pattern when the delay is larger than the spike length (as is normally the case), resulting in phase-locked pulses with a modal structure in spectrum.

In this paper we put forward the idea of combining the HB-SASE and the optical klystron concepts using standard chicanes with the dual objective of enhancing the longitudinal coherence of the produced radiation while reducing the FEL saturation length. The delay of the chicanes is used to improve the brightness of the FEL radiation using the HB-SASE concept, while the longitudinal dispersion is employed to reduce the saturation length via the optical klystron effect. In particular, we propose to use monotonously decreasing delays along the undulator beamline around the optimum value that maximizes the optical klystron effect.[2] Our strategy is to start with a more or less periodic decrease of the delays along the beamline and to finish with rather small delays. By taking different delay values we efficiently fill the gaps of the power profile between the radiation spikes, thereby conveniently increasing the coherence based on the HB-SASE concept. Using different delays also avoids the onset of sidebands in the spectrum profile that would appear if the same delay were used in all chicanes. Moreover, this delay configuration allows us to take advantage of the optical klystron effect in an efficient way, since the delays are kept around the optimum value of the optical klystron configuration. Finally, by finishing with small delays we avoid the overbunching at the end of the beamline that would deteriorate the FEL performance – if rather large delays were used close to saturation of the FEL process, where the bunching is close to maximum, the beam would be overbunched and as a consequence the FEL emission would be limited. Our approach is to select the optimum delay configuration based on both the brightness and the saturation length, but giving a higher weight to the coherence improvement. Considering that different delay sequences will provide an equivalent result in brightness, a possibility is to choose from these cases the one giving the shortest saturation length.

As mentioned before, the change in microbunching caused by the longitudinal dispersion of the standard chicanes will reduce the achievable brightness with respect to an optimized HB-SASE scheme with isochronous chicanes. The maximum coherence improvement will be about a factor of ten with respect to the standard SASE case, still significantly far from the Fourier limit. Since the maximum brightness with standard chicanes is already limited, in our scheme it is not worth or necessary to employ undulator modules significantly shorter than the gain length. The fact that the CHB-SASE scheme uses compact chicanes and does not require very short undulator modules makes it efficient in terms of FEL performance. In general, undulator modules with a length around the FEL gain length will be sufficient, but an individual optimization of the module length will be required for a given FEL facility. As an example, Prat *et al.* (2016) found for the soft X-ray beamline of SwissFEL that, at a radiation wavelength of 1 nm, the achievable brightness no longer improves when reducing the undulator length to less than 2 m. Moreover, shorter undulator modules would compromise the FEL efficiency due to a poor filling factor.

A merit of the proposed scheme is its simplicity. Only standard compact chicanes between undulator modules are required, and extremely short undulator modules are avoided. To be as compact as possible, the dipole magnets should be permanent and not electromagnetic. As an example, the permanent-magnet chicanes designed for the soft X-rays of SwissFEL (Ganter, 2017; Prat *et al.*, 2016) occupy only 20 cm and are able to delay up to 5 fs an electron beam with an energy of 3 GeV, sufficient for the implementation of the CHB-SASE scheme. This kind of chicane can be placed at any inter-undulator section of a standard FEL facility without significantly increasing the total length of the beamline.

3. Simulation results

The simulations are performed for the soft X-ray beamline of SwissFEL (Ganter, 2017), planned to deliver FEL radiation with wavelengths between 0.7 and 5 nm to scientific users from 2020. We carry out the numerical calculations with the code *Genesis 1.3* (Reiche, 1999) for four different wavelengths: 0.7 nm, 1 nm, 3 nm and 5 nm. The electron beam parameters are the following: the current profile is flat with a current value of 2 kA and a total duration of 100 fs (corresponding to a bunch charge of 200 pC), the maximum beam energy is 3.4 GeV, the slice energy spread is 0.5 MeV, the normalized emittance is 400 nm, and the average β-function in the undulator is 10 m. The undulator modules are 2 m long, they have a period of 38 mm and the maximum field parameter K is 3.5. We consider a beamline with up to 18 undulator modules. Each inter-undulator section is 0.72 m long, including among other components the magnetic chicane and a quadrupole magnet to focus the beam. For radiation wavelengths of 0.7, 1 and 3 nm, the beam energy has a maximum value of 3.4 GeV, with the K value adapted to fit the corresponding resonant condition. For the wavelength of 5 nm, we take a maximum K value of 3.5 and reduce the beam energy to 2.6 GeV to match the resonant wavelength. This is the tuning scheme foreseen at SwissFEL to match the resonant condition for different wavelength values.

First of all we find the optimum delays for the distributed optical klystron configuration. We scan the delays, which are the same for all the chicanes, from 0 to 5 fs in steps of 0.33 fs. In principle the ultimate optimization of the saturation length based on the optical klystron effect would require different delay values for the chicanes along the undulator beamline (larger at the beginning and smaller afterwards). For our purposes, however, obtaining the optimum by using the same

[2] Prat *et al.* (2016) have already suggested using the HB-SASE scheme with dispersive chicanes and decreasing delays to take advantage of the optical klystron effect. In that work, however, we optimized the brightness increase and the saturation length independently. Here we propose to simultaneously optimize the FEL brightness and the saturation length.

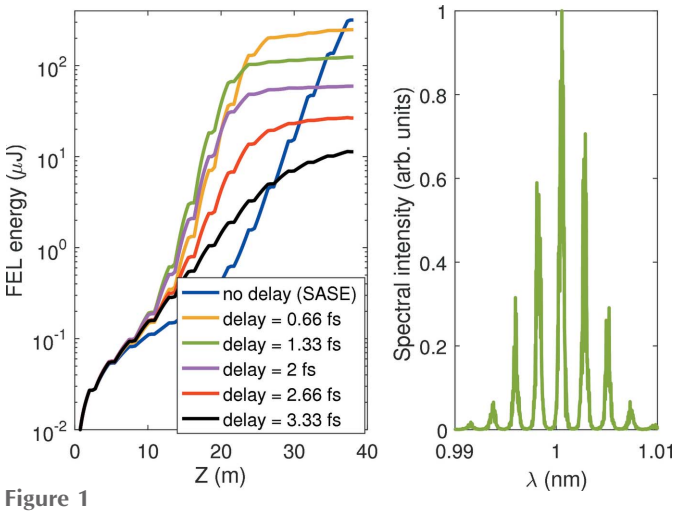

Figure 1
Left: average FEL pulse energy along the undulator beamline for different distributed delays in optical klystron configuration for a radiation wavelength of 1 nm (for the sake of readability not all simulated cases are shown). Right: average spectrum at FEL saturation for the delay giving the minimum saturation length (1.33 fs).

delay for all chicanes before FEL saturation is sufficient. Fig. 1 shows, as an example for a wavelength of 1 nm, the FEL pulse energy along the undulator beamline for some of the applied delay sequences, together with the average spectrum at saturation for the optimum case. As shown by the figure, the spectrum presents strong sidebands around the central radiation wavelength. The delay for the shortest saturation length is 1 fs for a radiation wavelength of 0.7 nm, 1.33 fs for a wavelength of 1 nm, 4.33 fs for 3 nm and 4.66 fs for 5 nm. As expected, the optimum delay increases with the radiation wavelength (Ding *et al.*, 2006).

We then perform simulations for CHB-SASE with numerous delay configurations. We try 20 or more delay sequences for each radiation wavelength. In each sequence the delays are decreasing along the undulator beamline and start with values around the obtained optimum for the optical klystron configuration. For each delay configuration we average the results over ten simulations with different random seeds for the electrons' shot noise. We select the best delay sequence for each wavelength, as mentioned before, giving higher importance to the brightness than to the saturation length. Fig. 2 shows for the central wavelength of 3 nm the spectral bandwidth and the FEL pulse energy along the undulator beamline for different CHB-SASE cases using different delays sequences, together with the SASE and the optimum optical klystron configurations.

Table 1 lists the saturation lengths and the spectral bandwidth at saturation for the best CHB-SASE case in comparison with the standard SASE configuration. Figs. 3–6 show for the different central wavelengths the FEL pulse energy along the undulator beamline and the spectrum profile at saturation for the CHB-SASE and SASE cases. For a better comparison of the performance we define a measure for the saturation length as the position where the FEL pulse energy reaches a certain value, close to the saturation point. We choose this value to be 200 μJ for the shorter radiation wavelengths (0.7 and 1 nm) and 500 μJ for the longer wavelengths (3 and 5 nm). In comparison with SASE, the saturation length for the CHB-SASE case is reduced by about 8 m for wavelengths of 0.7 and 1 nm, about 7 m for 3 nm wavelength, and 6 m for a wavelength of 5 nm. This is equivalent to three undulator modules for the short wavelengths. In percentage terms, the saturation length is reduced by approximately 20% for the short wavelengths (0.7 nm 1 nm) and by about 25% for the

Table 1
Relative FWHM bandwidth at saturation, and saturation length for SASE and CHB-SASE.

	SASE	CHB-SASE
0.7 nm		
Bandwidth	16.9×10^{-4}	1.9×10^{-4}
Saturation length (m)	47.3	39.3
1 nm		
Bandwidth	21.0×10^{-4}	2.3×10^{-4}
Saturation length (m)	36.4	28.1
3 nm		
Bandwidth	34.9×10^{-4}	6.4×10^{-4}
Saturation length (m)	26.3	19.1
5 nm		
Bandwidth	37.0×10^{-4}	13.5×10^{-4}
Saturation length (m)	23.0	17.2

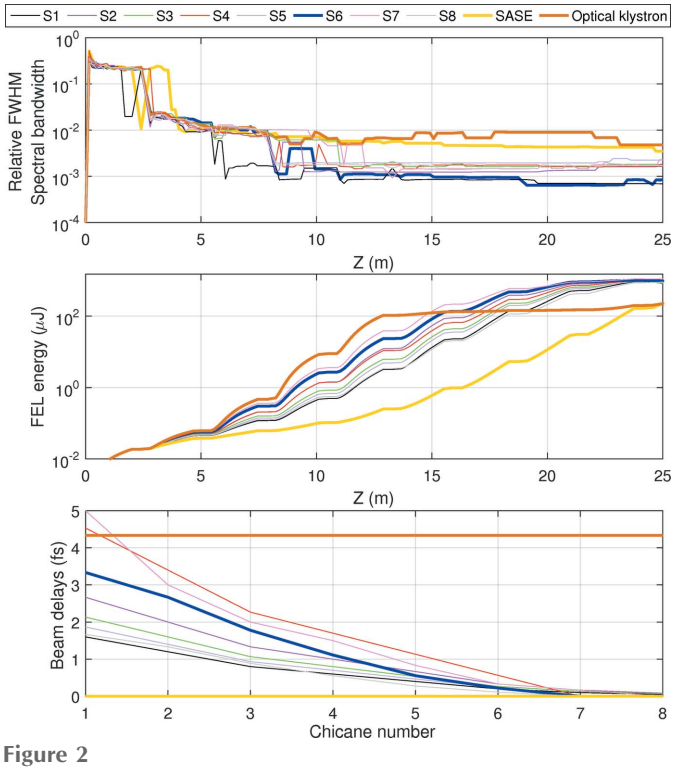

Figure 2
Spectral bandwidth (top plot) and FEL pulse energy (center plot) along the beamline for a radiation wavelength of 3 nm for different configurations: standard SASE, optimum optical klystron and CHB-SASE with different delay sequences (S1 to S8). The delays of each sequence are shown in the bottom plot. Sequence 6 (S6) was taken as the optimum one. For the sake of readability not all simulated cases are shown.

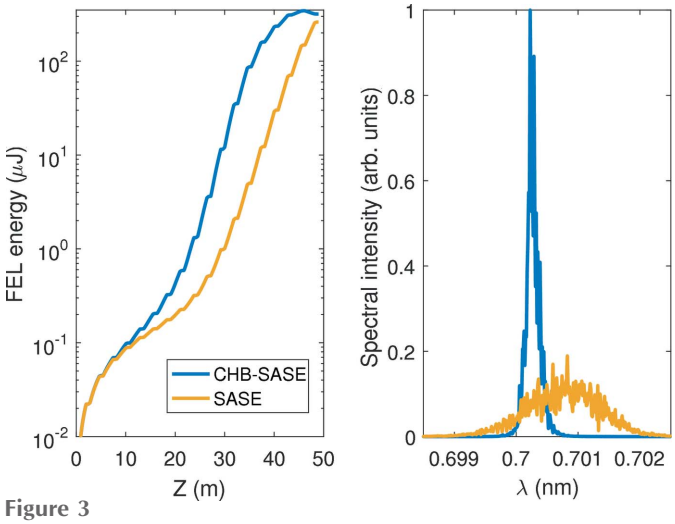

Figure 3
FEL pulse energy and spectrum profile at saturation for a central wavelength of 0.7 nm for CHB-SASE and the standard SASE cases. Both the FEL pulse energy and the spectrum are averages over ten simulations.

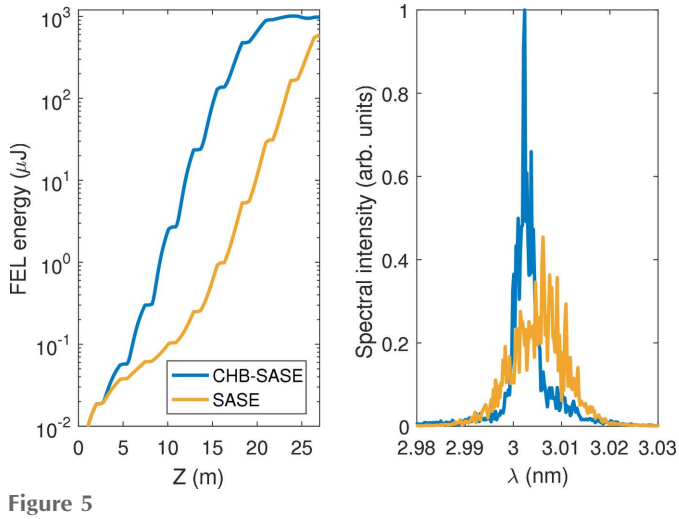

Figure 5
FEL pulse energy and spectrum profile at saturation for a central wavelength of 3 nm for CHB-SASE and the standard SASE cases. Both the FEL pulse energy and the spectrum are averages over ten simulations.

long wavelengths (3 and 5 nm). The saturation length could be further reduced with a pure optical klystron optimization but, as mentioned above, at the expense of a low-quality spectrum with sidebands.

For the shorter wavelengths (0.7 and 1 nm) the improvement in bandwidth with respect to SASE is about a factor of ten – still about one order of magnitude away from transform-limited pulses and equivalent to what was obtained earlier (Prat *et al.*, 2016) for a wavelength of 1 nm. The bandwidth enhancement is reduced to a factor of about five for a wavelength of 3 nm and to approximately a factor of three for the longest wavelength of 5 nm. Moreover, the pedestal around the central wavelength is worse for longer wavelengths. The deteriorated performance for the longer wavelengths is because the gain length in these cases is shorter but the delays are still applied only every 2 m. Going to shorter undulator modules would not significantly improve the performance for the short wavelengths [as seen by Prat *et al.* (2016)] but it would enhance the efficiency for the long wavelengths. For the soft X-ray beamline of SwissFEL, however, we decided to not have undulator modules shorter than 2 m based on cost and filling-factor considerations. An alternative solution to have a better performance would be to diminish the gain length for the long wavelengths, for instance by increasing the slice energy spread of the beam with the laser heater or by increasing the β-function in the undulator.

Fig. 7 shows the optimum delays for the CHB-SASE and optical klystron schemes for all considered wavelengths. We observe that for short wavelengths (0.7 and 1 nm) the best performance is obtained when the first delay is about a factor of two larger than the optical klystron optimum, while for longer wavelengths it is better to start with shorter delays than with the best optical klystron delay. We obtain a better performance when the decrease in delay is rather linear along

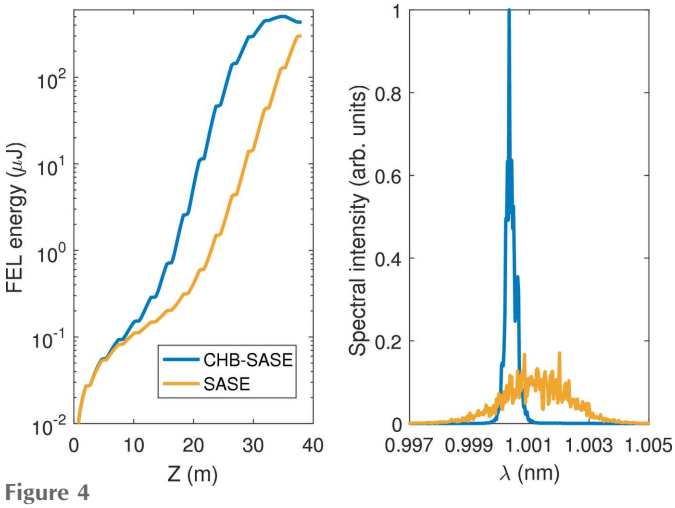

Figure 4
FEL pulse energy and spectrum profile at saturation for a central wavelength of 1 nm for CHB-SASE and the standard SASE cases. Both the FEL pulse energy and the spectrum are averages over ten simulations.

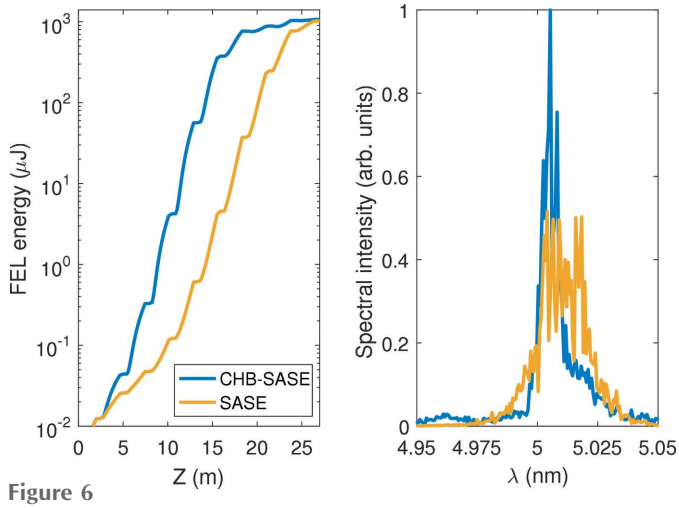

Figure 6
FEL pulse energy and spectrum profile at saturation for a central wavelength of 5 nm for CHB-SASE and the standard SASE cases. Both the FEL pulse energy and the spectrum are averages over ten simulations.

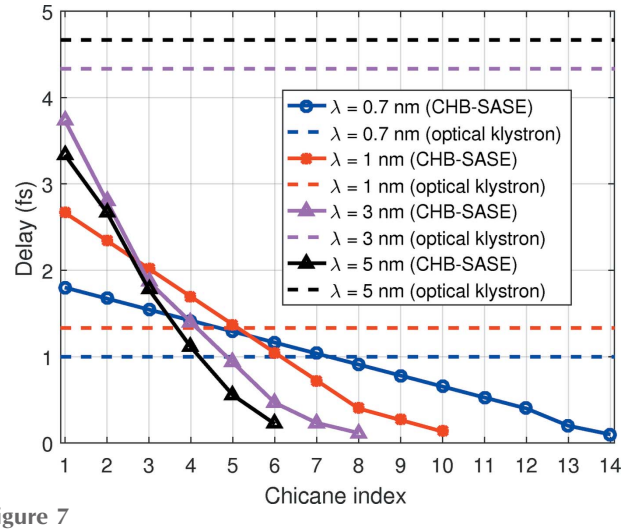

Figure 7
Optimum delays for the CHB-SASE and optical klystron schemes for the different wavelengths considered.

the beamline, except for the last chicanes for which the delays should go gently to zero delay to avoid overcompression and to fill the gaps between the radiation spikes. The integrated delays are between 10 and 13.5 fs for the different wavelengths, about an order of magnitude shorter than the total bunch length, indicating that the coherence is not imprinted over the whole length of the bunch.

4. Conclusion

We have presented a simple method that uses small chicanes to improve the longitudinal coherence of the SASE-FEL radiation within a compact beamline. The method combines the HB-SASE scheme and the optical klystron concept to optimize simultaneously the FEL brightness and saturation length. Simulation results for the soft X-ray beamline of SwissFEL show that, in comparison with SASE, the brightness can be improved by up to a factor of ten and that the required length to achieve saturation is reduced by at least 20%. Installing small chicanes between the undulator modules could be a feature for the next generation of FELs to enhance in a simple way both the FEL brightness and the saturation length. The space investment of installing the chicanes is more than compensated by the reduced saturation length, while providing narrower spectra than standard SASE.

Acknowledgements

The authors acknowledge Thomas Schietinger for fruitful discussions and for carefully proofreading the manuscript.

References

Ackermann, W., Asova, G., Ayvazyan, V., Azima, A., Baboi, N., Bähr, J., Balandin, V., Beutner, B., Brandt, A. & Bolzmann, A. (2007). *Nat. Photon.* **1**, 336–342.

Allaria, E., Appio, R., Badano, L., Barletta, W. A., Bassanese, S., Biedron, S. G., Borga, A., Busetto, E., Castronovo, D., Cinquegrana, P., Cleva, S., Cocco, D., Cornacchia, M., Craievich, P., Cudin, I., D'Auria, G., Dal Forno, M., Danailov, M. B., De Monte, R., De Ninno, G., Delgiusto, P., Demidovich, A., Di Mitri, S., Diviacco, B., Fabris, A., Fabris, R., Fawley, W., Ferianis, M., Ferrari, E., Ferry, S., Froehlich, L., Furlan, P., Gaio, G., Gelmetti, F., Giannessi, L., Giannini, M., Gobessi, R., Ivanov, R., Karantzoulis, E., Lonza, M., Lutman, A., Mahieu, B., Milloch, M., Milton, S. V., Musardo, M., Nikolov, I., Noe, S., Parmigiani, F., Penco, G., Petronio, M., Pivetta, L., Predonzani, M., Rossi, F., Rumiz, L., Salom, A., Scafuri, C., Serpico, C., Sigalotti, P., Spampinati, S., Spezzani, C., Svandrlik, M., Svetina, C., Tazzari, S., Trovo, M., Umer, R., Vascotto, A., Veronese, M., Visintini, R., Zaccaria, M., Zangrando, D. & Zangrando, M. (2012). *Nat. Photon.* **6**, 699–704.

Allaria, E., Castronovo, D., Cinquegrana, P., Craievich, P., Dal Forno, M., Danailov, M. B., D'Auria, G., Demidovich, A., De Ninno, G., Di Mitri, S., Diviacco, B., Fawley, W. M., Ferianis, M., Ferrari, E., Froehlich, L., Gaio, G., Gauthier, D., Giannessi, L., Ivanov, R., Mahieu, B., Mahne, N., Nikolov, I., Parmigiani, F., Penco, G., Raimondi, L., Scafuri, C., Serpico, C., Sigalotti, P., Spampinati, S., Spezzani, C., Svandrlik, M., Svetina, C., Trovo, M., Veronese, M., Zangrando, D. & Zangrando, M. (2013). *Nat. Photon.* **7**, 913–918.

Amann, J., Berg, W., Blank, V., Decker, F.-J., Ding, Y., Emma, P., Feng, Y., Frisch, J., Fritz, D., Hastings, J., Huang, Z., Krzywinski, J., Lindberg, R., Loos, H., Lutman, A., Nuhn, H.-D., Ratner, D., Rzepiela, J., Shu, D., Shvyd'ko, Y., Spampinati, S., Stoupin, S., Terentyev, S., Trakhtenberg, E., Walz, D., Welch, J., Wu, J., Zholents, A. & Zhu, D. (2012). *Nat. Photon.* **6**, 693–698.

Bonifacio, R., Pellegrini, C. & Narducci, L. M. (1984). *Opt. Commun.* **50**, 373–378.

Clarke, J., Angal-Kalinin, D., Bliss, N., Buckley, R., Buckley, S., Cash, R., Corlett, P., Cowie, L., Cox, G., Diakun, G., Dunning, D. J., Fell, B. D., Gallagher, A., Goudket, P., Goulden, A. R., Holland, D. M. P., Jamison, S. P., Jones, J. K., Kalinin, A. S., Liggins, W., Ma, L., Marinov, K. B., Martlew, B., McIntosh, P. A., McKenzie, J. W., Middleman, K. J., Militsyn, B. L., Moss, A. J., Muratori, B. D., Roper, M. D., Santer, R., Saveliev, Y., Snedden, E., Smith, R. J., Smith, S. L., Surman, M., Thakker, T., Thompson, N. R., Valizadeh, R., Wheelhouse, A. E., Williams, P. H., Bartolini, R., Martin, I., Barlow, R., Kolano, A., Burt, G., Chattopadhyay, S., Newton, D., Wolski, A., Appleby, R. B., Owen, H. L., Serluca, M., Xia, G., Boogert, S., Lyapin, A., Campbell, L., McNeil, B. W. J. & Paramonov, V. V. (2014). *J. Instrum.* **9**, T05001.

Ding, Y., Emma, P., Huang, Z. & Kumar, V. (2006). *Phys. Rev. ST Accel. Beams*, **9**, 070702.

Emma, P., Akre, R., Arthur, J., Bionta, R., Bostedt, C., Bozek, J., Brachmann, A., Bucksbaum, P., Coffee, R., Decker, F., Ding, Y., Dowell, D., Edstrom, S., Fisher, A., Frisch, J., Gilevich, S., Hastings, J., Hays, G., Hering, P., Huang, Z., Iverson, R., Loos, H., Messerschmidt, M., Miahnahri, A., Moeller, S., Nuhn, H., Pile, G., Ratner, D., Rzepiela, J., Schultz, D., Smith, T., Stefan, P., Tompkins, H., Turner, J., Welch, J., White, W., Wu, J., Yocky, G. & Galayda, J. (2010). *Nat. Photon.* **4**, 641–647.

Feldhaus, J., Saldin, E. L., Schneider, J. R., Schneidmiller, E. A. & Yurkov, M. V. (1997). *Opt. Commun.* **140**, 341–352.

Ferray, M., L'Huillier, A., Li, X. F., Lompre, L. A., Mainfray, G. & Manus, C. (1988). *J. Phys. B At. Mol. Opt. Phys.* **21**, L31–L35.

Ganter, R. (2017). *Athos Conceptual Design Report.* Technical Report. Paul Scherrer Institute, Villigen, Switzerland.

Geloni, G., Kocharyan, V. & Saldin, E. (2011). *Extension of Self-Seeding to Hard X-rays>10 keV as a Way to Increase User Access at the European XFEL.* Report 11-224. Deutsches Elektronen-Synchrotron, Hamburg, Germany.

Geloni, G., Kocharyan, V. & Saldin, E. (2015). *Scheme to Increase the Output Average Spectral Flux of the European XFEL at 14.4 keV.* Report 15-141. Deutsches Elektronen-Synchrotron, Hamburg, Germany.

Geloni, G. K. V. & Saldin, E. (2010). *A simple method for controlling the line width of SASE X-ray FELs.* Report 10-053. Deutsches Elektronen-Synchrotron, Hamburg, Germany.

Ishikawa, T., Aoyagi, H., Asaka, T., Asano, Y., Azumi, N., Bizen, T., Ego, H., Fukami, K., Fukui, T., Furukawa, Y., Goto, S., Hanaki, H., Hara, T., Hasegawa, T., Hatsui, T., Higashiya, A., Hirono, T., Hosoda, N., Ishii, M., Inagaki, T., Inubushi, Y., Itoga, T., Joti, Y., Kago, M., Kameshima, T., Kimura, H., Kirihara, Y., Kiyomichi, A., Kobayashi, T., Kondo, C., Kudo, T., Maesaka, H., Maréchal, X. M., Masuda, T., Matsubara, S., Matsumoto, T., Matsushita, T., Matsui, S., Nagasono, M., Nariyama, N., Ohashi, H., Ohata, T., Ohshima, T., Ono, S., Otake, Y., Saji, C., Sakurai, T., Sato, T., Sawada, K., Seike, T., Shirasawa, K., Sugimoto, T., Suzuki, S., Takahashi, S., Takebe, H., Takeshita, K., Tamasaku, K., Tanaka, H., Tanaka, R., Tanaka, T., Togashi, T., Togawa, K., Tokuhisa, A., Tomizawa, H., Tono, K., Wu, S., Yabashi, M., Yamaga, M., Yamashita, A., Yanagida, K., Zhang, C., Shintake, T., Kitamura, H. & Kumagai, N. (2012). *Nat. Photon.* **6**, 540–544.

Kang, H., Min, C., Heo, H., Kim, C., Yang, H., Kim, G., Nam, I., Baek, S. Y., Choi, H., Mun, G., Park, B. R., Suh, Y. J., Shin, D. C., Hu, J., Hong, J., Jung, S., Kim, S., Kim, K., Na, D., Park, S. S., Park, Y. J., Han, J., Jung, Y. G., Jeong, S. H., Lee, H. G., Lee, S., Lee, S., Lee, W., Oh, B., Suh, H. S., Parc, Y. W., Park, S., Kim, M. H., Jung, N., Kim, Y., Lee, M., Lee, B., Sung, C., Mok, I., Yang, J., Lee, C., Shin, H., Kim, J. H., Kim, Y., Lee, J. H., Park, S., Kim, J., Park, J., Eom, I., Rah, S., Kim, S., Nam, K. H., Park, J., Park, J., Kim, S., Kwon, S., Park, S. H., Kim, K. S., Hyun, H., Kim, S. N., Kim, S., Hwang, S., Kim, M. J., Lim, C., Yu, C., Kim, B., Kang, T., Kim, K., Kim, S., Lee, H., Lee, H., Park, K., Koo, T., Kim, D. & Ko, I. S. (2017). *Nat. Photon.* **11**, 708–713.

Kondratenko, A. M. & Saldin, E. L. (1980). *Part. Accel.* **10**, 207–216.

McNeil, B. W. J., Thompson, N. R. & Dunning, D. J. (2013). *Phys. Rev. Lett.* **110**, 134802.

Pellegrini, C., Marinelli, A. & Reiche, S. (2016). *Rev. Mod. Phys.* **88**, 015006.

Penco, G., Allaria, E., De Ninno, G., Ferrari, E. & Giannessi, L. (2015). *Phys. Rev. Lett.* **114**, 013901.

Prat, E., Calvi, M., Ganter, R., Reiche, S., Schietinger, T. & Schmidt, T. (2016). *J. Synchrotron Rad.* **23**, 861–868.

Prat, E. & Reiche, S. (2018). *J. Synchrotron Rad.* **25**, 329–335.

Ratner, D., Abela, R., Amann, J., Behrens, C., Bohler, D., Bouchard, G., Bostedt, C., Boyes, M., Chow, K., Cocco, D., Decker, F. J., Ding, Y., Eckman, C., Emma, P., Fairley, D., Feng, Y., Field, C., Flechsig, U., Gassner, G., Hastings, J., Heimann, P., Huang, Z., Kelez, N., Krzywinski, J., Loos, H., Lutman, A., Marinelli, A., Marcus, G., Maxwell, T., Montanez, P., Moeller, S., Morton, D., Nuhn, H. D., Rodes, N., Schlotter, W., Serkez, S., Stevens, T., Turner, J., Walz, D., Welch, J. & Wu, J. (2015). *Phys. Rev. Lett.* **114**, 054801.

Reiche, S. (1999). *Nucl. Instrum. Methods Phys. Res. A*, **429**, 243–248.

Saldin, E. L., Schneidmiller, E. A., Shvyd'ko, Y. V. & Yurkov, M. V. (2001). *Nucl. Instrum. Methods Phys. Res. A*, **475**, 357–362.

Saldin, E. L., Schneidmiller, E. A. & Yurkov, M. V. (2002). *Opt. Commun.* **202**, 169–187.

Saldin, E. L., Schneidmiller, E. A. & Yurkov, M. V. (2003). *The Free Electron Laser Klystron Amplifier Concept.* Report 03-108. Deutsches Elektronen-Synchrotron, Hamburg, Germany.

Schneidmiller, E. A. & Yurkov, M. V. (2012). *Phys. Rev. ST Accel. Beams*, **15**, 080702.

Schneidmiller, E., Faatz, B., Kuhlmann, M., Rönsch-Schulenburg, J., Schreiber, S., Tischer, M. & Yurkov, M. (2017). *Phys. Rev. Accel. Beams*, **20**, 020705.

Stupakov, G. (2009). *Phys. Rev. Lett.* **102**, 074801.

Vinokurov, N. A. & Skrinsky, N. A. (1977). Report BINP 77-59. Budker Institute for Nuclear Physics, Novosibirsk, Russia.

Wu, J., Marinelli, A. & Pellegrini, C. (2013*a*). *Proceedings of the 34th International Free-Electron Laser Conference (FEL2012)*, 26–31 August 2012, Nara, Japan, pp. 237–240. TUPD07.

Wu, J., Pellegrini, C., Marinelli, A., Nuhn, H.-D., Decker, F.-J., Loos, H., Lutman, A., Ratner, D., Feng, Y., Krzywinski, J., Zhang, D. & Zhu, D. (2013*b*). *Proceedings of the 4th International Particle Accelerator Conference (IPAC2013)*, 12–17 May 2013, Shanghai, China, pp. 2068–2070. WEODB101.

Xiang, D., Ding, Y., Huang, Z. & Deng, H. (2013). *Phys. Rev. ST Accel. Beams*, **16**, 010703.

Yu, L. H. (1991). *Phys. Rev. A*, **44**, 5178–5193.